Reprinted from July, 1983, Vol. 105, Journal of Vibration, Stress, and Reliability in Design

# Design of Direct-Drive Mechanical Arms'

**Haruhiko Asada**[2]
Visiting Research Scientist of Robotics Institute.
Assoc Mem. ASME

**Takeo Kanade**
Senior Research Scientist.

Computer Science Department and Robotics Institute.
Carnegie-Mellon University.
Schenley Park,
Pittsburgh. Penn. 15213

*This paper describes the design concept of a new robot based on the direct-drive method using rare-earth d-c torque motors. Because these motors have high torque, light weight and compact size, we can construct robots with far better performance than those presently available. For example, we can eliminate all the transmission mechanisms, such as reducers and chain belts, between the motors and their loads, and construct a simple mechanism (direct-drive) where the arm links are directly coupled to the motor rotors. This elimination can lead to excellent performance: no backlash, low friction, low inertia, low compliance and high reliability, all of which are suited for high-speed, high-precision robots. First we propose a basic configuration of direct-drive robots. Second a general procedure for designing direct-drive robots is shown, and the feasibility of direct drive for robot actuation is discussed in terms of weights and torques of joints. One of the difficulties in designing direct-drive robots is that motors to drive wrist joints are loads for motors to drive elbow joints, and they are loads for motors at shoulders. To reduce this increasing series of loads is an essential issue for designing practical robots. We analyze the joint mass system for simplified kinematic model of the direct-drive robots, and show how the loads are reduced significantly by using rare-earth motors with light-weight and high torque. We also discuss optimum kinematic structures with minimum arm weight. Finally, we describe the direct-drive robotic manipulator (CMU arm) developed at Carnegie-Mellon University, and verify the design theory.*

## 1 Introduction

Present electrically powered manipulators are still far inferior to human arms and unsatisfactory for many applications in terms of speed, accuracy and versatility. One of the reasons for this poor performance comes from the transmission mechanisms, such as gear trains, lead screws, steel belts, chains, and linkages, which are used to transmit power from the motors to the load and to increase the driving torque. The following problems result from having complicated transmission mechanisms:

- Dynamic response is poor because of the heavy weight and/or high compliance of the transmission.
- Fine movements and pure torque control are difficult because of the relatively large friction and backlash at the transmission.
- Additional complicated mechanisms for minimizing the backlash are necessary and they need careful adjustment and regular maintenance.

One of the main reasons for using a transmission mechanism with a high gear reduction ratio is that the conventional servo motors provide rather small torque and high speed. Recently, however, high-torque and low-speed motors using new rare-earth magnetic materials (eg. samarium cobalt) have been developed and are becoming available for industrial use [1,2]. Since the maximum magnetic energy product is 3 to 10 times larger than with a conventional ferrite or alnico magnet, the performance of the rare-earth d-c motors can be improved greatly. Such motors have a high

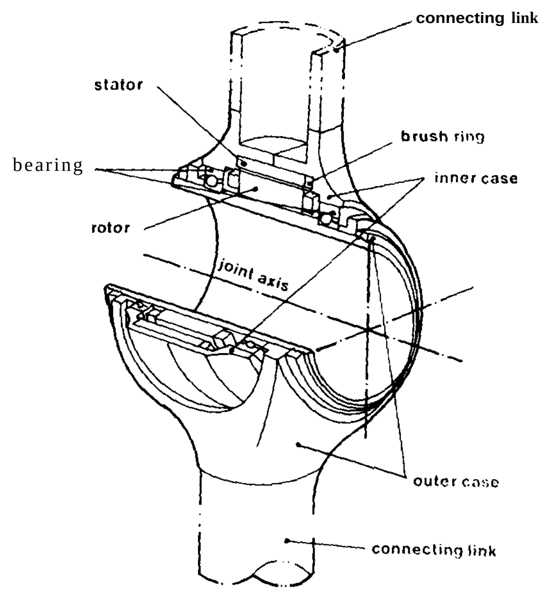

Fig. 1 A direct-drive joint

'This research was supported in part by Carnegie-Mellon University and in part by Office of Naval Research, N00014-79-C0661.

'Research Associate of Automation Research Laboratory, Kyoto University, Japan.

Contributed by the Design Engineering Division for publication in the JOURNAL OF MECHANICAL DESIGN. Manuscript received at ASME Headquarters September 29, 1981; revised manuscript received October 23, 1981.

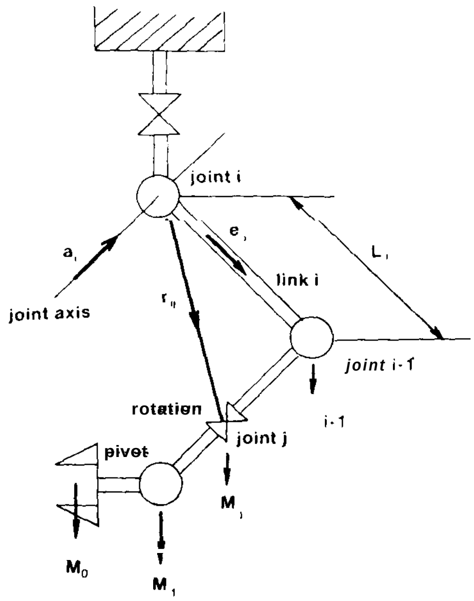


Fig. 2 Kinematic model of a direct-drive manipulator

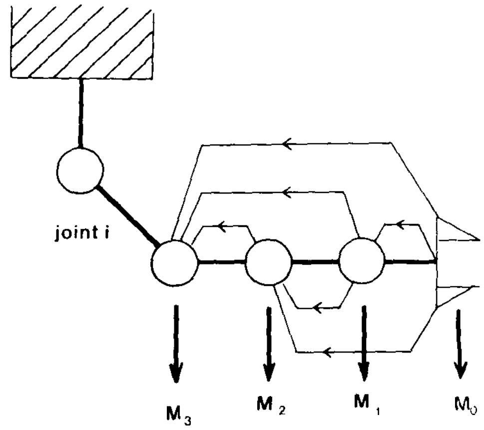


Fig. 3 Relations of loads to joints

output torque, low speed, light weight, and compact body. They are suited for the manipulator drive and will allow elimination of the transmission mechanism.

In this paper, we discuss a manipulator where all the joint axes are directly coupled to rotors of rare-earth magnet d-c torque motors in order to obtain excellent features: no backlash, low friction, low compliance, and high reliability. First a basic configuration of direct-drive manipulators is shown. Second, we present a design theory for direct drive manipulators by using a simple kinematic model. We then find an arm structure most suitable for direct drive. Finally, we describe a direct-drive manipulator developed at Carnegie-Mellon University, and verify the theoretical result.

## 2 Configuration of Direct-Drive Manipulators

Basically, a direct-drive manipulator consists of a series of active joints whose typical construction is shown in Fig. 1. The outer case, in the figure, rotates against the inner case and about the joint axis. The inner and outer cases are connected to the other joints by connecting links. The motor illustrated is a d-c torque motor which consists of a rotor, a stator, and a brush ring. The stator and the brush ring are installed in the inner case, while the rotor is directly coupled to the outer case without any transmission mechanism.

Some variations are possible in the joint mechanism. For example, the stator can be attached to the outer case, and the rotor to the inner case. Also, when the joint axis is parallel to the connecting links, the location of the motor and bearings are different from the layout shown. In any case, the joint has a simple structure with all the components attached directly to the inner and outer cases.

Since the direct drive method eliminates all the transmission mechanisms and since the load is directly coupled to the actuator output, a direct-drive manipulator is essentially free from the problems caused by transmission mechanisms. For example, backlash is essentially removed, and compliance is almost zero except at the connecting links. Slight Coulomb friction can exist but only at the bearings supporting the joint axis.

Because of its simple structure, a direct-drive manipulator is composed of a much smaller number of mechanical parts. This is another important advantage of direct drive, because it potentially improves the reliability of the manipulator and makes it free from complex maintenance or readjustment.

Although the direct drive of a manipulator is expected to provide a number of excellent improvements in performance, there are some problems inherent in this design. One of the difficulties in developing a direct-drive manipulator is that the motors to drive wrist joints are themselves loads for the motors at elbow joints which are also loads for the motors at shoulder joints. In other words, the load increases rapidly along a series of active joints and this load may lead to an impractical design requiring excessively large motors to drive a heavy arm. An essential issue in designing a practical manipulator is to reduce this increasing load. To achieve this reduction we will analyze the series of joint loads and discuss the feasibility of direct drive in the manipulator actuation.

## 3 Theory for Designing Direct-Drive Manipulators

**3.1 *Kinematic Model.*** To analyze a series of joint loads we first derive a kinematic model of direct-drive manipulators. Since the motors are directly coupled to joint axes without including any transmission mechanism, a direct-drive manipulator inevitably has the motors attached at the joint. As the weight of connecting links is light in comparison with the joints, almbst all mass of the arm is concentrated at each joint, which consists of a motor, bearings and a housing. Figure 2 shows a simplified kinematic model of direct-drive manipulators, where we assume:

- The arm consists of a series of points mass $M_j$ connected by straight links without mass.
- The joint axes, illustrated by arrows in the figure, are perpendicular or parallel to the links which they connect.

Each joint is numbered 1 to $n$ from the tip to the base. We call a joint whose axis is perpendicular to the links a pivot, and a joint whose axis is parallel to the links a rotation. In Fig. 2, the first joint is a pivot and the second a rotation.

The position vector from joint $i$ to joint $j$ $(i>j)$ is given as follows,

$$\mathbf{r}_{ij} = \sum_{k=j+1}^{i} l_k \mathbf{e}_k \tag{1}$$

where $l_k$ is the length of link $k$ between joints $k-1$ and $k$, and $\mathbf{e}_k$ is a unit vector which points to the direction of link $k$. The unit vector $\mathbf{e}_k$ depends on joint angles $\theta_k, \ldots, \theta_n$.

About the axis of joint $i$, the moment $Tg_i$ is developed due to the gravity force of the external load $M_0$ and a series of point mass from $M_1$ through $M_{i-1}$. The moment $Tg_i$ is given as follows:

$$Tg_i = \mathbf{a}_i \cdot \sum_{j=0}^{i-1} (\mathbf{r}_{ij} \times \mathbf{g}) M_j \tag{2}$$

**Table 1** Series of joint mass **for all-pivotal-joint arms**

$\bar{\alpha} = 0.1$

| joint mass / $\bar{\beta}$ | $\bar{M}_1$ | $\bar{M}_2$ | $\bar{M}_3$ | $\bar{M}_4$ | $\bar{M}_5$ | $\bar{M}_6$ | total ($\Sigma \bar{M}_i$) |
|---|---|---|---|---|---|---|---|
| 1 | 1.10 | 3.61 | 10.51 | 30.12 | 86.09 | 246.04 | 378.47 |
| 0.5 | 0.55 | 1.50 | 3.44 | 7.57 | 16.50 | 35.93 | 66.48 |
| 0.25 | 0.28 | 0.68 | 1.33 | 2.44 | 4.38 | 7.82 | 17.92 |

**Table 2 Series of joint mass for various kinematic structures**

$\bar{\alpha} = 0.1 \quad \bar{\beta} = 0.5$

| joint mass / (tip) structure (base) | $\bar{M}_1$ | $\bar{M}_2$ | $\bar{M}_3$ | $\bar{M}_4$ | $\bar{M}_5$ | $\bar{M}_6$ | total |
|---|---|---|---|---|---|---|---|
| R-P-R-P-P-P | 0* | 1.20 | 1.20 | 4.24 | 9.08 | 19.68 | 36.41 |
| R-P-P-R-P-P | 0 | 1.20 | 2.61 | 2.61 | 9.22 | 19.76 | 36.40 |
| R-P-P-P-R-P | 0 | 1.20 | 2.61 | 5.68 | 5.68 | 20.06 | 36.22 |
| R-P-P-P-P-R | 0 | 1.20 | 2.61 | 5.68 | 12.34 | 2.60** | 25.43 |
| P-R-P-R-P-P | 0.55 | 0.55 | 2.61 | 2.61 | 9.08 | 19.46 | 35.86 |
| P-R-P-P-R-P | 0.55 | 0.55 | 2.61 | 5.61 | 5.61 | 19.76 | 35.69 |
| P-R-P-P-P-R | 0.55 | 0.55 | 2.61 | 5.61 | 12.17 | 2.60 | 25.09 |
| P-P-R-P-R-P | 0.55 | 1.50 | 1.50 | 5.68 | 5.68 | 19.68 | 35.59 |
| P-P-R-P-P-R | 0.55 | 1.50 | 1.50 | 5.68 | 12.17 | 2.73 | 25.12 |
| P-P-P-R-P-R | 0.55 | 1.50 | 3.44 | 3.44 | 12.34 | 3.05 | 25.32 |
| R-P-R-P-R-P | 0 | 1.20 | 1.20 | 4.24 | 4.24 | 14.69 | 26.57 |
| R-P-P-R-P-R | 0 | 1.20 | 2.61 | 2.61 | 9.22 | 2.31 | 18.95 |
| R-P-R-P-P-R | 0 | 1.20 | 1.20 | 4.24 | 9.08 | 2.06 | 18.78 |
| P-R-P-R-P-R | 0.55 | 0.55 | 2.61 | 2.61 | 9.08 | 2.32 | 18.72 |

R: Rotational joint P: Pivotal joint
*) Since we assume that the external load is a point mass, the required torque for the rotational joint at the arm tip becomes zero.
**) The joint axis of the rotational joint at the base is assumed to be parallel to the direction of gravity. Then the gravity load becomes zero in this case.

where $\mathbf{a}_i$ denotes a unit vector which points to the direction of the axis of joint $i$, $\mathbf{g}$ denotes an acceleration vector of gravity, and $\times$ and $\circ$ stand respectively for vector and inner products.

The moment of inertia of the arm about the axis of joint $i$ is

$$I_i = \sum_{j=0}^{i-1} M_j |\mathbf{r}_{ij} \times \mathbf{a}_i|^2 \tag{3}$$

where $|\circ|$ denotes a vector norm. $Tg_i$ and $I_i$ depend on joint angles $\theta_i$'s because they include $\mathbf{r}_{ij}$.

**3.2 Series of Joint Mass.** In designing a direct-drive manipulator, maximum torque of each active joint is one of the basic specifications that we should consider. Let us suppose that, for an arbitrary arm configuration, the maximum torque of the active joint $Tm_i$ must be larger than that required to rotate the joint with a specified angular acceleration $\alpha_i$. The maximum torque must also bear the gravity force of the arm. Namely,

$$Tm_i = \max_{\theta_1, \ldots, \theta_n} \{Tg_i + I_i \alpha_i\} \tag{4}$$

All the mass of joints from 1 through $i-1$ need to be predetermined to compute the above maximum torque, because $Tg_i$ and $I_i$ include $M_j$ for $1 \le j \le i-1$. Therefore the design of the arm drive system should be carried out step by step starting from joint 1 ton.

1. Give a maximum external load $M_0$, and set $i = 1$.
2. Compute the maximum required torque $Tm_i$ by equations (2–4).
3. Select a motor which can develop $Tm_i$ and determine the joint mass $M_i$ after designing the joint housing.
4. Set $i = i + 1$, and go back to step 2 while $i \le n$.

As we noted, the active joint $i$ is itself a load for joint $i+1$, and both are loads for joint $i+2$, and so on. If joint $i$ is heavy in comparison with its output torque, active joint $i+1$ needs to be more powerful and therefore tends to be heavier; this chain is multiplicative. Hence, the required torques for the subsequent active joint increase very fast. Therefore, light weight (as well as high output torque) is an essential requirement for active joints in a direct-drive manipulator.

This observation suggests that we introduce $\beta$, the ratio of mass to peak torque ($M/T$ ratio), as an index to evaluate the active joint performance

$$\beta = \frac{M}{T} \tag{5}$$

where $T$ is maximum torque, and M is mass of the active joint.

Now, let us consider a special case where every link is of the same length, all the joints are pivots, and all the joints have the same $M/T$ ratio $\beta$. We can then express analytically a series of joints mass $M_i$ which satisfies equation (4). Notice that both the gravity load $Tg_i$ and the inertia load $I_i$ are maxima when the arm is kept at a level as shown in Fig. 3. The weight of motor $i$ is written in the following recursive formula:

$$\bar{M}_i = \bar{\beta} \sum_{j=0}^{i-1} [(i-j) + (i-j)^2 \bar{\alpha}] \bar{M}_j \tag{6}$$

where $\tilde\alpha$, $\tilde M_i$ and $\tilde\beta$ are made dimensionless by using link length $l$, maximum load $M_0$ and acceleration of gravity g,

$$\tilde\beta = \beta l g, \quad \tilde\alpha = \frac{l}{g}\alpha, \quad \tilde M_i = \frac{M_i}{M_0} \tag{7}$$

Figure 3 shows how joint mass relates to the previous joints; the dependency is shown by arrows. For example, $\tilde M_3$ depends on $\tilde M_2$, $\tilde M_1$ and $M_0$, while $\tilde M_2$ depends on $\tilde M_1$ and $\tilde M_0$, and $\tilde M_1$ depends on $\tilde M_0$. Since each arrow in the figure is associated with a conversion from required torque to mass of the active joint, $M_3$ consists of terms proportional to $\tilde\beta$, $\tilde\beta^2$ and $\tilde\beta^3$. In fact, the solution of equation (6) has the following form.

$$\tilde M_i = \sum_{k=1}^{i} \Big\{ \sum_{0=m_0<m_1 \ldots <m_k=i} \prod_{j=1}^{k} [(m_j - m_{j-1}) + (m_j - m_{j-1})^2 \tilde\alpha] \Big\} \tilde\beta^k \tag{8}$$

Table 1 shows $\tilde M_i$'s for $\tilde\alpha = 0.1$ and $\tilde\beta = 1$, 0.5, and 0.25. The joint mass increases exponentially with the joint number. When $\tilde\beta = 1$, the total arm weight is about 380 times heavier than that of an external object that the arm can carry. Direct drive is not feasible if an excessively large motor is required, or if the total weight is too large. If $\tilde\beta$ becomes 1/2, the total arm weight is drastically reduced to 1/6. The last joint, $\tilde M_6$ is reduced as much as 1/7. Thus small M/T ratio $\tilde\beta$ is very effective in reducing the series of joints mass.

**3.3 Suitable Arm Structure for Direct Drive.** The previous discussion assumed that all the joints were pivots. Now we discuss the case where some rotational joints are involved in a series of joints, and investigate how the series of joints mass can be reduced. Then we find out what kinematic arm structures are suitable for direct drive. Consider the case as shown in Fig. 4 where joint $i$ is a rotation instead of a pivot. Then, only joints from 1 to $i-2$ are the loads for active joint $i$, because the axis of joint $i$ penetrates the point mass $i-1$ and therefore the point mass $i-1$ is not a load for joint $i$. Thus the formula for $\tilde M_i$, in this case, is as follows,

$$\tilde M_i = \tilde\beta \sum_{j=0}^{i-2} [(i-j) + (i-j)^2 \tilde\alpha] \tilde M_j \tag{9}$$

Comparing this with equation (6), we note that the load for active joint $i$ is reduced. Moreover, the rotational joint $i$ can be placed at any position on links $i+1$ and $i$. If it is placed on joint $i+1$, joint $i$ is not a load for joint $i+1$. In addition, the joint $i$ can be a counter weight for joint $i+1$ if it is placed on the extension line of link $i+1$ in the direction from joint $i-1$ to joint $i+1$.

The adjacent joints of a rotational joint must be pivots, because two consecutive rotational joints are equivalent to one. Robot arms with 6 degrees of freedom can have at most three rotational joints, and there are 21 combinations in the arrangement of pivots and rotations. For each case the series of joint mass are computed. Table 2 lists mass of joints for several structures which contain at least 2 rotational joints. From this table we can conclude that the arm structure P-R-P-R-P-R from the tip to the shoulder is the lightest and that R-P-R-P-P-R is as light as P-R-P-R-P-R. They are therefore most suitable structures for direct drive.

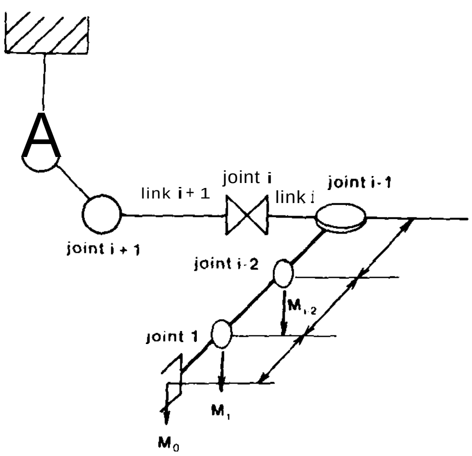


**Fig. 4 Rotational joint and its load**

## 4 Development of a Direct-Drive Manipulator

**4.1 Investigation of Motors.** The feasibility of developing a direct-drive manipulator depends on the performance of motors, which are the most important components in active joints. In reducing the $M/T$ ratio of the active joint, a motor with high torque and light weight is required. We therefore

**Table 3 Comparison of rareearth cobalt magnet and alnico magnet motors on market**

| class of size | magnet | dimensions* od** (mm) | id** (mm) | length (mm) | mass (kg) | peak torque (Nm) | MM/T ratio (kg/Nm) |
|---|---|---|---|---|---|---|---|
| small | rare earth | 81 | 29 | 60 | 1.52 | 6.8 | 0.224 |
| | alnico | 72 | 23 | 64 | 1.31 | 1.7 | 0.768 |
| medium | rare earth | 183 | 100 | 32 | 2.70 | 15.0 | 0.181 |
| | alnico | 183 | 100 | 34 | 3.05 | 8.2 | 0.374 |
| large | rare earth | 228 | 136 | 42 | 4.44 | 27.2 | 0.163 |
| | alnico | 228 | 136 | 41 | 4.34 | 14.9 | 0.291 |
| extra large | rare earth | 646 | 523 | 152 | 100.1 | 952 | 0.105 |
| | alnico | 734 | 415 | 165 | 100.1 | 585 | 0.171 |

* The dimensions are for motors with standard hubs and flanges

** od; outer diameter, id; inner diameter.

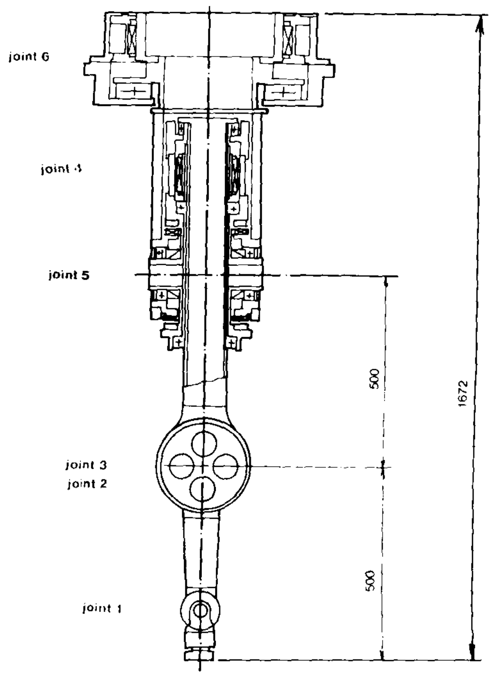


**Fig. 5 Drawing of CMU arm**

Table 4 Motors used for CMU Arm

| Joint # | 1 | 2 | 3 | 4 | 5 | 6 |
|---|---|---|---|---|---|---|
| peak toraue (Nm) | 6.8 | 6.8 | 54.4 | 81.6 | 136 | 204 |
| mass (Kg) | 1.52 | 1.52 | 8.88 | 19.6 | 23.8 | 32.6 |
| MM/T (kg/Nm) | 0.224 | 0.224 | 0.163 | 0.240 | 0.175 | 0.160 |
| diameter (mm) | 81 | 81 | 228 | 238 | 366 | 603 |
| permanent magnet | SmCo | SmCo | SmCo | Alnico | Alnico | Alnico |

investigate the ratio of mass of motor to peak torque (we call it MM/Tratio) for d-c torque motors in the market.

A permanent magnet with a high density of magnetic flux increases output torque thus reducing $MM/T$ ratio. Recently, we have seen rapid progress in technology of rare-earth cobalt magnetic materials. The maximum magnetic energy product of rare earth cobalt is 19 to 30 MGOe, while those of conventional ferrite magnet and alnico magnet are about 3 MGOe, and 5.5 MGOe. respectively.

Table 3 shows a comparison of $MM/T$ ratios for d-c torque motors on the market. The pairs of rare-earth and alnico magnet motors grouped in the table by thick lines have approximately the same shape and mass. However, the peak torque for the rare-earth magnet motors is about twice as large as that of alnico motors, and therefore the $MM/T$ ratio is reduced to 1/2. Also, the larger motor has the smaller $MM/T$ ratio. The extra large alnico magnet motor has a $MM/T$ ratio as small as that of the medium size rare-earth motors.

**4.2 CMU Arm.** A direct-drive manipulator (CMU Arm) was designed at Carnegie-Mellon University based on the above design theory. We now describe the outline of the design and verify the theory.

The first step in designing the manipulator was to provide basic specifications. They were as follows: Arm length is 1 m, maximum external load is 6 kg, number of joints is 6. The average link length is 1/6 m. Suppose that the standard $MM/T$ ratio of the motors is 0.18 kg/Nm, and the weight of bearings plus inner and outer cases is about 70 percent of that of the motors, then, from equation (7), we know the dimensionless $M/T$ ratio $\hat{\beta}$ of each joint as follows.

$$(0.18\,\mathrm{kg/Nm}) \times g \times (1+0.7) \times 1/6\ \mathrm{m} = 0.5$$

When we adopt the lightest arm structure P-R-P-R-P-R, the series of joint mass shown at the bottom row in Table 2 is obtained. The anticipated total arm mass in this case is

$$6\ \mathrm{kg} \times 18.72 = 112\ \mathrm{kg}.$$

This is a reasonable result in comparison with light-duty electrically powered robots on the market [3].

We then selected motors based on the above design outline. As we can see from Table 3, the MM/T ratio of alnico magnet motors, with the exception of the extra large motor, are far from the chosen standard value 0.18 kg/Nm. The rare-earth motors, however, satisfied the required standard and therefore we used them for driving some of the joints. The motors for driving the shoulder part must be large. As the larger diameter motors have the smaller $MM/T$ ratio, we can use alnico magnet motors for joint 5 and 6 without exceeding the standard 0.18 kg/Nm. In addition, the large diameter motors are not necessarily inconvenient for installing at the shoulder part.

The motors we used are listed in Table 4. Motors from 1 through 3 have rare-earth cobalt permanent magnets, and the others have alnico magnets. Table 2 shows that a very large motor is necessary for joint 5. The use of a counter weight can reduce the actual load for the joint 5. Namely, we locate the motor 4 on the other side of the forearm so that it plays the role of a counter weight. The required torque for the motor 5 is much reduced as listed in Table 4.

Figure 5 depicts a design drawing for the whole arm based on the above motor selection. Motor 2 is installed inside of joint 3 at the elbow part, motor 4 is above joint 5. The movable joint angles are 180 deg for a pivot and 360 deg for a rotation. The total arm weight is about 130 kg. The maximum speed at the arm tip is designed to be 4 m/s, which is the fastest speed of the present electrically-powered robots.

## 5 Conclusion

The direct-drive manipulator has a number of excellent features that the present electrically powered robotic manipulators do not have. However, the development of a practical manipulator requires powerful active joints with light weight. We analyzed required torques for a series of active joints by introducing ratio of mass to peak torque of active joints. We also found that the suitable kinematic structures for the direct drive are P-R-P-R-P-R and R-P-R-P-P-R in the case of robots with 6 degrees of freedom. The CMU direct-drive arm was designed according to these theoretical concepts and by using motors presently available on the market. Improvement in joint housings as well as more powerful motors will allow us to have robots of lighter weight and higher performance than the one currently available.


## Acknowledgments

The authors wish to express their gratitude to Raj Reddy for his constant encouragement and enthusiasm on this project.


## References


1 Ojima, T., et. al.. "Magnetic Properties of a New Type of Rare-Earth Cobalt Magnets." *IEEE Transactions on Magnetics,* Vol. MAG-13. No. 5, Sept. 1977, pp. 1317-1319.

2 Kano, T.. and Yanagida, H., *Rare Earths,* Gihodo Press, 1980, pp. 220-231.

3 Unimate PUMA Robot, *Technical Manual,* Unimation Inc., Apr. 1980.